Drug Discovery Hot Paper

International Edition: DOI: 10.1002/anie.201502763
German Edition: DOI: 10.1002/ange.201502763

Inhibition of Ras Signaling by Blocking Ras–Effector Interactions with Cyclic Peptides**

Punit Upadhyaya, Ziqing Qian, Nicholas G. Selner, Sarah R. Clippinger, Zhengrong Wu, Roger Briesewitz, and Dehua Pei**

Abstract: *Ras genes are frequently activated in human cancers, but the mutant Ras proteins remain largely "undruggable" through the conventional small-molecule approach owing to the absence of any obvious binding pockets on their surfaces. By screening a combinatorial peptide library, followed by structure–activity relationship (SAR) analysis, we discovered a family of cyclic peptides possessing both Ras-binding and cell-penetrating properties. These cell-permeable cyclic peptides inhibit Ras signaling by binding to Ras-GTP and blocking its interaction with downstream proteins and they induce apoptosis of cancer cells. Our results demonstrate the feasibility of developing cyclic peptides for the inhibition of intracellular protein–protein interactions and of direct Ras inhibitors as a novel class of anticancer agents.*

The monomeric GTPases K-Ras, H-Ras, and N-Ras play critical roles in many signaling pathways and regulate cell proliferation, differentiation, and survival.[1] Wild-type Ras oscillates between inactive GDP-bound (Ras-GDP) and active GTP-bound (Ras-GTP) forms, with the latter interacting with and activating multiple effector proteins, including Raf, PI3K, and Ral-GDS. Somatic mutations that cause constitutive activation of Ras are the most common activating lesions and are found in approximately 30% human cancers.[2] These mutations impair GTP hydrolysis, thereby increasing the Ras-GTP population and causing uncontrolled cell growth. Genetic studies suggest that blocking the Ras–effector protein interaction should have therapeutic benefits in cancer patients;[3,4] however, doing so pharmacologically has been challenging because the Ras protein surface has no obvious pockets for small-molecule drugs to bind.[5] Consequently, most of the drug-discovery efforts have so far been focused on inhibiting the signaling molecules downstream of Ras,[6] the posttranslational processing/membrane anchoring of Ras,[6,7] or the nucleotide exchange activity of Ras.[8–14] Inhibitors that physically block Ras–effector protein interactions have generally lacked potency, selectivity, and/or membrane permeability.[15,16] Herein, we report a family of cyclic peptides possessing both Ras-binding and cell-penetrating properties. These cell-permeable cyclic peptides bind potently to Ras-GTP near the effector-binding site and block its interaction with downstream proteins, thereby resulting in growth inhibition and apoptosis of cancer cells.

We previously reported a cyclic peptide inhibitor against K-Ras, compound **12** (Figure 1), which blocks the Ras–effector protein interaction in vitro but lacks cellular activity owing to poor membrane permeability.[16] Interestingly, compound **12** contains an amphipathic sequence motif, Arg-Arg-nal-Arg-Fpa (where Fpa is L-4-fluorophenylalanine and nal is D-β-naphthylalanine), which resembles a recently discovered cyclic cell-penetrating peptide (CPP).[17,18] To improve the potency and membrane permeability of compound **12**, we designed a second-generation library in which the CPP-like motif was retained, while the remaining structure was replaced with a random peptide sequence of 0–5 amino acids ($X^{1–5}$). The library (ca. 1.3×10^6 compounds) was constructed with 28 different amino acids[19] at the X^1–X^5 positions on spatially segregated TentaGel beads,[20] with each bead displaying a unique cyclic peptide on its surface and a linear peptide of the same sequence in its interior as an encoding tag (Figure 1). Because the effector-binding site of Ras is highly negatively charged,[21] we anticipated that screening the library against K-Ras might select one or more additional arginine and/or aromatic hydrophobic residues at the random positions which, together with the Arg-Arg-nal-Arg-Fpa motif, might generate a functional CPP.[17,18]

Screening of the peptide library against K-Ras(G12 V) identified 13 hits (Table S1 in Supporting Information). When assayed in solution by fluorescence anisotropy (FA), hits **4A**, **5A**, **7A**, **9A** (Figure 1), **12A**, and **13A** showed strong binding to K-Ras (Figure S1 in Supporting Information). In a homogeneous time-resolved fluorescence (HTRF) assay, hits **9A** and **12A** inhibited the Ras–Raf interaction with half maximal inhibitory concentration (IC_{50}) values of 0.65 and 1.0 μM, respectively (Figure 2a). Gratifyingly, hits **9A** and **12A** contained additional Trp and/or Arg residues in the X^2–X^5 region, were cell permeable, and exhibited weak antiproliferative activity against lung cancer cells (Figure S2). These two peptides were named cyclorasin (for cyclic Ras inhibitor) **9A** and **12A**, respectively.

[*] Dr. P. Upadhyaya, Dr. Z. Qian, Dr. N. G. Selner, S. R. Clippinger, Prof. Dr. Z. Wu, Prof. Dr. D. Pei
Department of Chemistry and Biochemistry
The Ohio State University
484 West 12th Avenue, Columbus, OH 43210 (USA)
E-mail: pei.3@osu.edu
Dr. R. Briesewitz
Department of Pharmacology, The Ohio State University
5065 Graves Hall, 333 West 10th Avenue, Columbus, OH 43210 (USA)
E-mail: Roger.Briesewitz@osumc.edu

[**] This work was supported by grants from the National Institutes of Health (GM062820, GM110208, and CA132855 to D.P.). We thank Prof. Andrea Doseff for helpful suggestions to some of the cellular tests.

Supporting information for this article is available on the WWW under http://dx.doi.org/10.1002/anie.201502763.

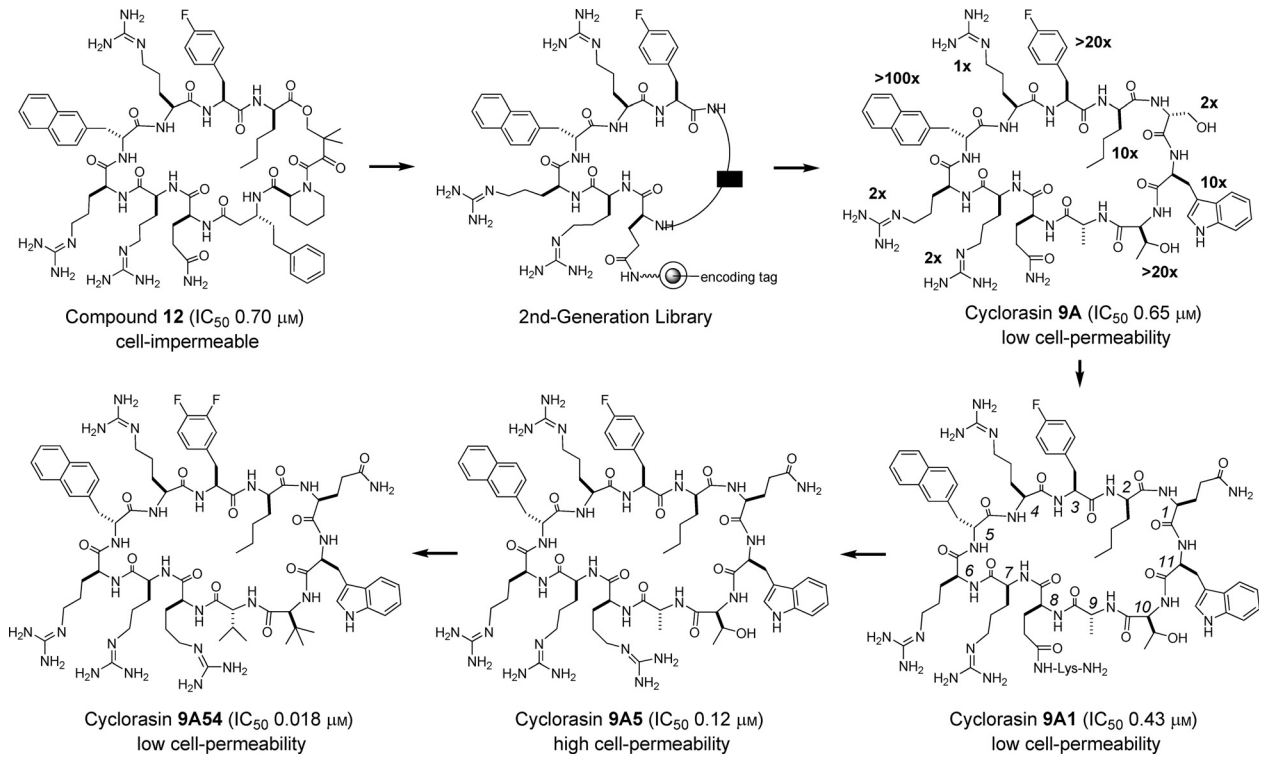

Figure 1. Flowchart showing the evolution of the cyclorasin Ras inhibitors. The numbers next to the structure of cyclorasin **9A** indicate activity loss upon replacing the corresponding residue with alanine (or D-alanine). The residue numbering shown in the structure of **9A1** is adopted for compounds **9A1** to **9A54**.

Because of its relatively high potency, cyclorasin **9A** was chosen for optimization. Alanine scan analysis revealed that nal, Fpa, Thr, norleucine (nle), and Trp are critical for K-Ras binding, since the replacement of any of these residues with L- or D-alanine reduced the Ras inhibitory activity by over 10-fold. Substitution of alanine for the remaining residues had relatively minor effects (less than 2-fold). Since the D-serine residue was not critical for Ras binding, it was replaced by an L-Gln to provide an alternative site for attachment to the solid support and was designated as position 1 (Figure 1). The resulting peptides (cyclorasins **9A1**–**4**), which contained different glutamine derivatives at position 8, had similar inhibitory activity against the Ras–Raf interaction (Table S2), thus suggesting that Gln8 is not critical for Ras binding. Gln8 was therefore replaced with L- or D-arginine to potentially improve the membrane permeability of the peptide.[17,18] To our delight, the resulting peptides (**9A5** and **9A6**) showed both improved cell permeability and an approximately 4-fold higher affinity for K-Ras ($IC_{50} = 0.12$ and 0.17 μM, respectively; Figure 2a). Further modifications of **9A5** and **9A6** produced mixed results, with a few resulting in significant improvements (Table S2). Replacement of the D-Ala at position 9 by D-valine (val9), Thr10 by L-*tert*-leucine (Tle), or Fpa3 by 3,4-difluorophenylalanine (F_2pa) increased the affinity by approximately 2-fold (**9A14**, **9A16**, and **9A43**, respectively). Finally, combinations of val9, Tle10, and F_2pa3 substitutions produced cyclorasins **9A51** and **9A54** as highly potent Ras inhibitors ($IC_{50} = 0.014$ and 0.018 μM, respectively; Figure 2a).

Peptides with strong K-Ras binding ($IC_{50} \leq 0.2$ μM) were tested for antiproliferative activity against H1299 lung cancer cells (Figure 2b). Cyclorasin **9A5** was the most potent ($LD_{50} \approx 3$ μM), whereas peptides with greater Ras binding affinities (e.g., 9A54) were less active in the 3-(4,5-dimethylthiazol-2-yl)-2,5-diphenyltetrazolium bromide (MTT) assay. To test whether poor membrane permeability limited the cellular activity of the latter peptides, we treated A549 lung cancer cells with fluorescein isothiocyanate (FITC)-labeled **9A5** or **9A54** and examined the internalization of the peptides by confocal microscopy (Figure 2c). Cells treated with FITC-**9A5** exhibited intense diffuse fluorescence throughout the cytoplasm, whereas cells treated with FITC-**9A54** showed much weaker and predominantly punctate fluorescence, which is indicative of endosomal entrapment. Flow cytometry analysis showed that FITC-**9A5** entered the lung cancer cells approximately 5-fold more efficiently than FITC-**9A54** (Figure 2d).

Cyclorasin **9A5** was selected to investigate the mechanism of the observed antiproliferative activity. The ability of **9A5** to inhibit the Ras–Raf interaction suggests that it binds to Ras-GTP. To test whether it is selective for Ras-GTP, we prepared K-Ras G12V loaded with GTP, GDP, or GPPNP (a non-hydrolyzable GTP analogue) and tested them for binding to FITC-**9A5** by FA. FITC-**9A5** bound to the Ras-GTP, Ras-GPPNP, and Ras-GDP with K_D values of 0.44, 0.64, and 2.5 μM, respectively (Note that labeling with FITC required the replacement of Arg6 with a lysine, which reduced its affinity for K-Ras; Figure 2e and Figure S3). FITC-**9A5** also bound to wild-type K- and H-Ras (which were mixtures of

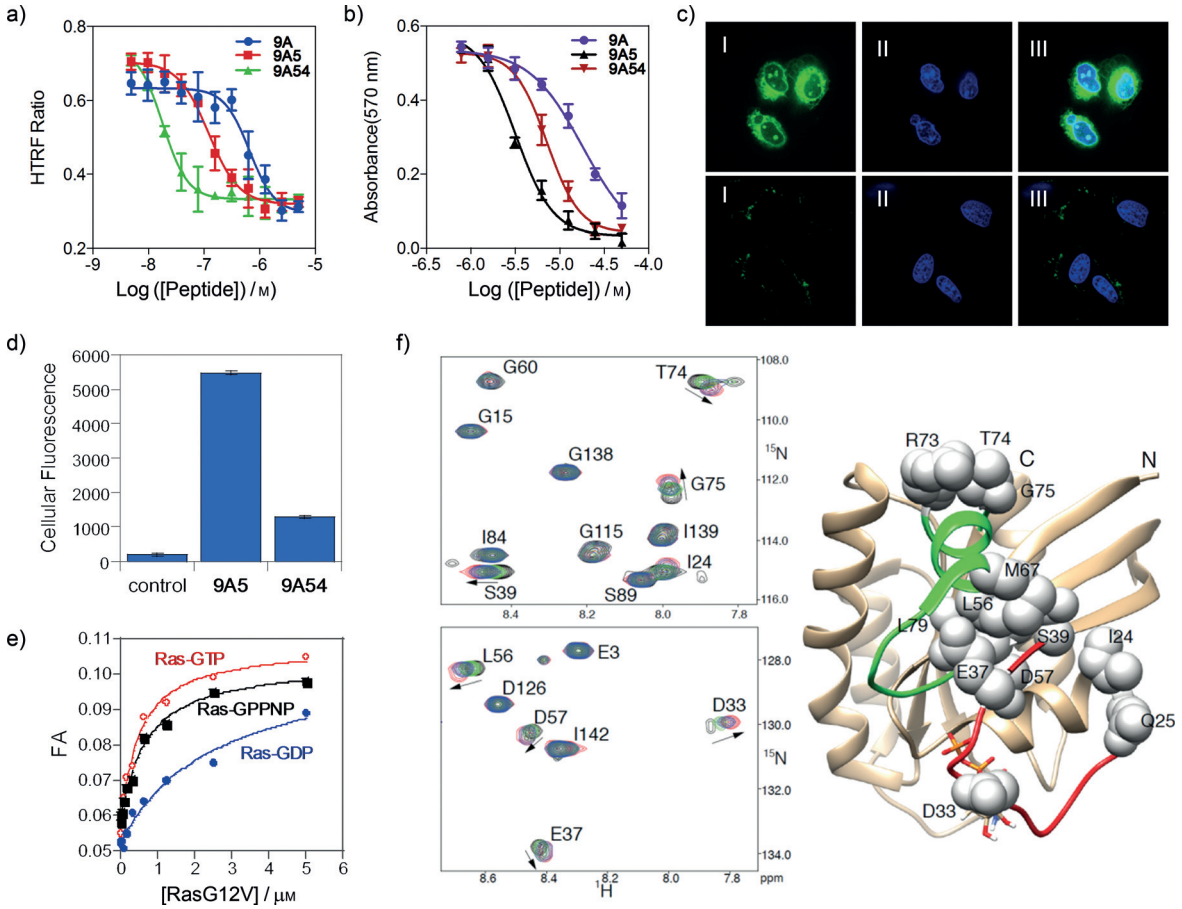

Figure 2. K-Ras binding, cellular uptake, and antiproliferative activity of cyclic peptides. a) HTRF assay of inhibition of the Ras–Raf interaction by **9A**, **9A5**, and **9A54**. b) Effect of **9A**, **9A5**, and **9A54** on H1299 cell viability, as measured by MTT assay. c) Live-cell confocal microscopic images of A549 cells treated with 5 μM FITC-**9A5** (top panels) or FITC-**9A54** (bottom panels) for 30 min. I: FITC fluorescence, II: nuclear stain with DRAQ5, and III: merge of I and II. d) Mean fluorescence of cells without treatment (control) or treated with FITC-**9A5** or FITC-**9A54**, as determined by flow cytometry. e) Binding of FITC-**9A5** to Ras-GTP, Ras-GDP, and Ras-GPPNP, as monitored by FA. f) Overlay of ^{1}H-^{15}N HSQC spectra of K-Ras(G12V)-GDP in the presence of 0 (black), 0.5 equiv (green), 0.75 equiv (blue), and an excess (red) of **9A5** at 298 K. K-Ras residues perturbed by **9A5** are mapped to the structure of wild-type K-Ras-GDP (4LPK) and shown as spheres. The switch I and II regions are colored red and green, respectively, and GDP is shown as a stick model.

GTP- and GDP-bound forms) with apparent K_D values of 1.2 and 1.4 μM, respectively, but not to a panel of five arbitrarily selected control proteins ($K_D \geq 30$ μM; Figure S3). Cyclorasin **9A5** is therefore a selective ligand of Ras-GTP.

To map the binding site of **9A5**, ^{15}N-labeled K-Ras-GPPNP was mixed with increasing concentrations of **9A5** and analyzed by ^{1}H-^{15}N heteronuclear single quantum correlation (HSQC) NMR spectroscopy (Figure 2 f). Unfortunately, most of the switch I and II residues were invisible in the HSQC spectra (Figure S4). K-Ras residues that exhibited detectable chemical shift perturbation upon binding to **9A5** include Gln25, Thr74, and Gly75. We therefore repeated the HSQC experiment with K-Ras-GDP. Most of the K-Ras residues were unaffected by **9A5**, thus indicating that binding of **9A5** does not induce global changes in the K-Ras structure (Figure S5). K-Ras residues that underwent detectable spectral shifts include Ile24, Gln25, Asp33, Glu37, and Ser39, which are within the switch I loop, the primary binding site of effector proteins[21] (Figure 2 f). The other perturbed residues (Leu56, Asp57, Met67, Arg73, Thr74, Gly75, and Leu79) are clustered around a small pocket between the switch I and II loops, which had previously been found to bind to small-molecule ligands.[9,10] The overlapping binding sites of **9A5** and Ras effector proteins are consistent with the observed inhibition of the Ras–Raf interaction by **9A5**.

The Raf/MEK/ERK and PI3K/PDK1/Akt signaling pathways represent the signature events downstream of Ras.[1] To determine whether **9A5** inhibits intracellular Ras activity, H358 lung cancer cells were treated with increasing concentrations of **9A5** and the Ras–Raf interaction was examined by precipitating the cell lysate with an anti-Ras antibody and immunoblotting with an anti-B-Raf antibody (Figure 3 a). In the absence of **9A5**, B-Raf co-precipitated with Ras. However, treatment of the cells with **9A5** dose-dependently inhibited the Ras–B-Raf interaction. Next, we examined Akt, MEK, and ERK1/2 phosphorylation in H1299 cells (Figure 3 b). Cyclorasin **9A5** inhibited EGF-stimulated phosphorylation of Akt at Thr308 and MEK in a dose-dependent manner ($IC_{50} \approx 3$ μM) and abolished the phosphorylation events at or above 12 μM, while the total Akt and MEK

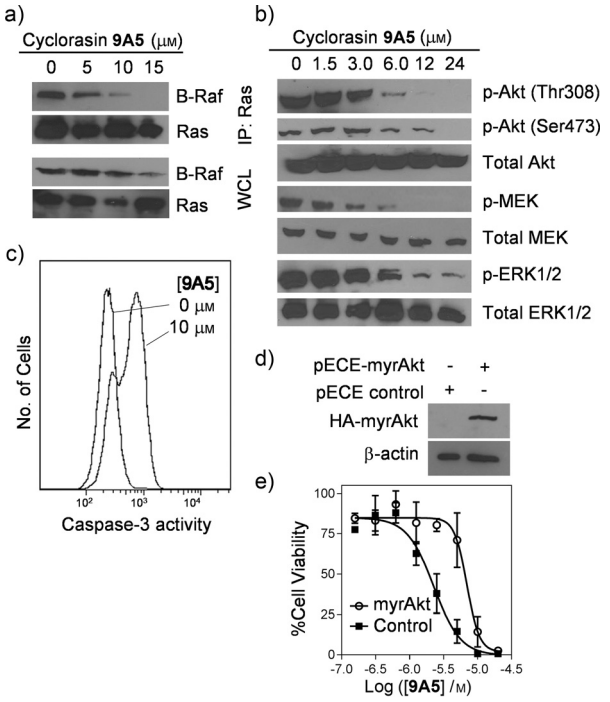

Figure 3. Inhibition of Ras signaling by **9A5**. a) Inhibition of the Ras–B-Raf interaction in H358 cells by **9A5**. WCL = whole-cell lysate. b) Dose-dependent inhibition of Akt, MEK, and ERK phosphorylation in H1299 cells by **9A5**. Cells were treated with the indicated concentrations of **9A5** for 10 min and stimulated with EGF (50 ng mL^{-1}) for 5 min before lysis. c) Activation of caspase-3 activity in H1299 cells by **9A5** (10 μM treatment for 3 h) as monitored by anti-caspase-3 immunostaining and flow cytometry. d,e) Protection of H1299 cells against **9A5**-induced apoptosis through ectopic expression of a constitutively active, HA-tagged, and myristoylated Akt (HA-myrAkt). The pECE control plasmid contains a frame-shift mutation in the myrAkt gene and the myrAkt protein levels in the cells were determined by immunoblotting with an anti-HA antibody. Actin was used as a loading control. Cell viability was determined by MTT assay and calculated relative to that of untreated cells.

protein levels remained constant. **9A5** also decreased the phosphorylation of ERK1/2 and Akt at Ser473, but less effectively, as expected from the fact that ERK1/2 functions downstream of MEK, and Akt Ser473 is phosphorylated by mTOR instead of PDK1.[22] A time-course experiment showed that the dephosphorylation of MEK and Akt was largely complete after 10 min of exposure to **9A5**, whereas a comparable degree of dephosphorylation of ERK was reached after 20 min (Figure S6a). H358 and H1299 cells express mutant K-Ras G12C and mutant N-Ras Q61K, respectively. Cyclorasin **9A5** also reduced MEK and Akt phosphorylation in lung cancer cell lines H1975 and H1650, which express wild-type Ras proteins but mutant EGFR (Figure S6b).

Dual inhibition of MEK and PI3K signaling results in a synergistic decrease in cell viability and increase in apoptosis of Ras-mutant cancer cells.[23–25] Given its ability to inhibit both the Raf/MEK/ERK and PI3K/PDK1/Akt pathways, **9A5** is expected to inhibit cell growth and induce apoptosis of cancer cells. Indeed, treatment of H1299 cells with 10 μM **9A5** for 3 h resulted in a 2.3-fold increase in the activity of caspase-3, a protease that plays a central role in apoptosis.(Figure 3c). Flow cytometry analysis of the treated cells showed positive staining with FITC-conjugated annexin V and propidium iodide, which stain apoptotic and dead cells, respectively (Figure S7). The treated cells also underwent morphological changes including cell rounding and reduction in cell size. Consistent with these morphological changes, LIM domain kinase and cofilin, which function downstream of Ras and regulate the assembly and disassembly of actin filaments, showed decreased phosphorylation upon treatment with **9A5**. Finally, transfection of H1299 cells with a constitutively active form of Akt[26] rendered the cells substantially less sensitive to **9A5**, with a median lethal dose (LD_{50}) value of around 8 μM, whereas transfection with a nonfunctional Akt gene had no effect (Figure 3d,e). Taken together, our data suggest that cyclorasin **9A5** is able to enter human cancer cells and bind directly to Ras proteins, thereby blocking Ras–effector protein interactions and causing cell growth inhibition and apoptosis, although we cannot rule out potential off-target effects that may also contribute to the observed cell growth inhibition and apoptotic cell death.

In summary, we have developed a family of cell-permeable cyclic peptides as potent and selective inhibitors of Ras-GTP by screening a peptide library followed by preliminary SAR studies. These peptides bind directly to Ras-GTP, thereby blocking its interaction with effector proteins and causing growth inhibition and apoptosis of cancer cells. Our compounds are among the first biologically active Ras inhibitors that act by physically blocking Ras–effector protein interactions. With sizes similar to that of cyclosporine A (an orally available cyclic peptide drug), these cyclic peptides should serve as useful leads for further development into therapeutic agents. Our strategy of integrating target-binding and cell-penetrating motifs into a single cyclic peptide should be applicable to the development of biologically active inhibitors against other intracellular protein–protein interactions.

Keywords: cancer · cell-penetrating peptides · cyclic peptides · protein–protein interactions · Ras signaling

How to cite: *Angew. Chem. Int. Ed.* **2015**, *54*, 7602–7606
Angew. Chem. **2015**, *127*, 7712–7716

[1] a) A. E. Karnoub, R. A. Weinberg, *Nat. Rev. Mol. Cell Biol.* **2008**, *9*, 517–531; b) A. Young, J. Lyons, A. L. Miller, V. T. Phan, I. R. Alarcon, F. McCormick, *Adv. Cancer Res.* **2009**, *102*, 1–17; c) P. M. Campbell, C. J. Der, *Semin. Cancer Biol.* **2004**, *14*, 105–114.

[2] I. A. Prior, P. D. Lewis, C. A. Mattos, *Cancer Res.* **2012**, *72*, 2457–2467.

[3] S. Gupta, A. R. Ramjaun, P. Haiko, Y. Wang, P. H. Warne, B. Nicke, E. Nye, G. Stamp, K. Alitalo, J. Downward, *Cell* **2007**, *129*, 957–968.

[4] E. Castellano, C. Sheridan, M. Z. Thin, E. Nye, B. Spencer-Dene, M. E. Diefenbacher, C. Moore, M. S. Kumar, M. M. Murillo, E. Gronroos, F. Lassailly, G. Stamp, J. Downward, *Cancer Cell* **2013**, *24*, 617–630.

[5] a) W. Wang, G. Fang, J. Rudolph, *Bioorg. Med. Chem. Lett.* **2012**, *22*, 5766–5776; b) J. Spiegel, P. M. Cromm, G. Zimmermann, T. N. Grossmann, H. Waldmann, *Nat. Chem. Biol.* **2014**, *10*, 613–

622; c) A. G. Stephen, D. Esposito, R. K. Bagni, F. McCormick, *Cancer Cell* **2014**, *25*, 272 – 281.
[6] a) S. Gysin, M. Salt, A. Young, F. McCormick, *Genes Cancer* **2011**, *2*, 359 – 372; b) A. T. Baines, D. Xu, C. J. Der, *Future Med. Chem.* **2011**, *3*, 1787 – 1808.
[7] G. Zimmermann, B. Papke, S. Ismail, N. Vartak, A. Chandra, M. Hoffmann, S. A. Hahn, G. Triola, A. Wittinghofer, P. I. Bastiaens, H. Waldmann, *Nature* **2013**, *497*, 638 – 642.
[8] A. G. Taveras, S. W. Remiszewski, R. J. Doll, D. Cesarz, E. C. Huang, P. Kirschmeier, B. N. Parmanik, M. E. Snow, Y.-S. Wang, J. d. del Rosario, B. Vibulbhan, B. B. Bauer, J. E. Brown, D. Carr, J. Catino, C. A. Evans, V. Girijavallabhan, L. Heimark, L. James, S. Liberles, C. Nash, L. Perkins, M. M. Senior, A. Tsarbopoulos, A. K. Ganguly, R. Aust, E. Brown, D. Delisle, S. Fuhrman, T. Hendrickson, C. Kissinger, R. Love, W. Sisson, E. Villafranca, S. E. Webber, *Bioorg. Med. Chem.* **1997**, *5*, 125 – 133.
[9] T. Maurer, L. S. Garrenton, A. Oh, K. Pitts, D. J. Anderson, N. J. Skelton, B. P. Fauber, B. Pan, S. Malek, D. Stokoe, M. J. Ludlam, K. K. Bowman, J. Wu, A. M. Giannetti, M. A. Starovasnik, I. Mellman, P. K. Jackson, J. Rudolph, W. Wang, G. Fang, *Proc. Natl. Acad. Sci. USA* **2012**, *109*, 5299 – 5304.
[10] Q. Sun, J. P. Burke, J. Phan, M. C. Burns, E. T. Olejniczak, A. G. Waterson, T. Lee, O. W. Rossanese, S. W. Fesik, *Angew. Chem. Int. Ed.* **2012**, *51*, 6140 – 6143; *Angew. Chem.* **2012**, *124*, 6244 – 6247.
[11] A. Patgiri, K. K. Yadav, P. S. Arora, D. Bar-Sagi, *Nat. Chem. Biol.* **2011**, *7*, 585 – 587.
[12] J. M. Ostrem, U. Peters, M. L. Sos, J. A. Wells, K. M. Shokat, *Nature* **2013**, *503*, 548 – 551.
[13] S. M. Lim, K. D. Westover, S. B. Ficarro, R. A. Harrison, H. G. Choi, M. E. Pacold, M. Carrasco, J. Hunter, N. D. Kim, T. Xie, T. Sim, P. A. Jänne, M. Meyerson, J. A. Marto, J. R. Engen, N. S. Gray, *Angew. Chem. Int. Ed.* **2014**, *53*, 199 – 204; *Angew. Chem.* **2014**, *126*, 203 – 208.
[14] E. S. Leshchiner, A. Parkhitko, G. H. Bird, J. Luccarelli, J. A. Bel-lairs, S. Escudero, K. Opoki-Nsiah, M. Godes, N. Perrimon, L. D. Walensky, *Proc. Natl. Acad. Sci. USA* **2015**, *112*, 1761 – 1766.
[15] a) D. Barnard, H. Sun, L. Baker, M. S. Marshall, *Biochem. Biophys. Res. Commun.* **1998**, *247*, 176 – 180; b) J. Kato-Stankiewicz, I. Hakimi, G. Zhi, I. Serebriiskii, L. Guo, H. Edamatsu, H. Koide, S. Menon, R. Ecki, S. Sakamuri, Y. Liu, Q.-Z. Chen, S. Agarwal, W. R. Baumbach, E. A. Golemis, F. Tamanoi, V. Khazak, *Proc. Natl. Acad. Sci. USA* **2002**, *99*, 14398 – 14403; c) V. González-Pérez, D. J. Reiner, J. K. Alan, C. Mitchell, L. J. Edwards, V. Khazak, C. J. Der, A. D. Cox, *J. Mol. Signaling* **2010**, *5*, 2; d) F. Shima, F. Shima, Y. Yoshikawa, M. Ye, M. Araki, S. Matsumoto, J. Liao, L. Hu, T. Sugimoto, Y. Ijiri, A. Takeda, Y. Nishiyama, C. Sato, S. Muraoka, A. Tamura, T. Osoda, K. Tsuda, T. Miyakawa, H. Fukunishi, J. Shimada, T. Kumasaka, M. Yamamoto, T. Kataoka, *Proc. Natl. Acad. Sci. USA* **2013**, *110*, 8182 – 8187; e) P. Upadhyaya, Z. Qian, N. A. A. Habir, D. Pei, *Tetrahedron* **2014**, *70*, 7714 – 7720.
[16] X. Wu, P. Upadhyaya, M. A. Villalona-Calero, R. Briesewitz, D. Pei, *MedChemComm* **2013**, *4*, 378 – 382.
[17] Z. Qian, T. Liu, Y. Y. Liu, R. Briesewitz, A. M. Barrios, S. M. Jhiang, D. Pei, *ACS Chem. Biol.* **2013**, *8*, 423 – 431.
[18] Z. Qian, J. R. LaRochelle, B. Jiang, W. Lian, R. L. Hard, N. G. Selner, R. Luechapanichkul, A. M. Barrios, D. Pei, *Biochemistry* **2014**, *53*, 4034 – 4046.
[19] The 28 amino acid set included 11 proteinogenic amino acids [Arg, Asp, Gln, Gly, His, Ile, Leu, Pro, Thr, Trp, and Tyr], 4 nonproteinogenic α-L-amino acids [L-4-fluorophenylalanine (Fpa), L-2-amino butyric acid (Abu), L-ornithine (Orn), and L-phenylglycine (Phg)], 9 α-D-amino acids [D-2-naphthylalanine (D-Nal), D-Ala, D-Asn, D-Glu, D-Lys, D-Nle, D-Phe, D-Ser and D-Val] and 4L-N^{α}-methylated amino acids [sarcosine (Sar), MeAla, MeLeu and MePhe].
[20] S. H. Joo, Q. Xiao, Y. Ling, B. Gopishetty, D. Pei, *J. Am. Chem. Soc.* **2006**, *128*, 13000 – 13009.
[21] M. E. Pacold, S. Suire, O. Perisic, S. Lara-Gonzalez, C. T. Davis, E. H. Walker, P. T. Hawkins, L. Stephens, J. F. Eccleston, R. L. Williams, *Cell* **2000**, *103*, 931 – 943.
[22] D. D. Sarbassov, D. A. Guertin, S. M. Ali, D. M. Sabatini, *Science* **2005**, *307*, 1098 – 1101.
[23] J. G. Shelton, L. S. Steelman, E. R. White, J. A. McCubrey, *Cell Cycle* **2004**, *3*, 372 – 379.
[24] M. L. Sos, S. Fischer, R. Ullrich, M. Peifer, J. M. Heuckmann, M. Koker, S. Heynck, I. Stuckrath, J. Weiss, F. Fisher, K. Michel, A. Goel, L. Regales, K. A. Politi, S. Perera, M. Getlik, L. C. Heukamp, S. Ansen, T. Zander, R. Beroukhim, H. Kashkar, K. M. Shokat, W. R. Sellers, D. Rauh, C. Orr, K. P. Hoeflich, L. Friedman, K. K. Wong, W. Pao, R. K. Thomas, *Proc. Natl. Acad. Sci. USA* **2009**, *106*, 18351 – 18356.
[25] J. A. Engelman, L. Chen, X. Tan, K. Crosby, A. R. Guimaraes, R. Upadhyay, M. Maira, K. McNamara, S. A. Perera, Y. Song, L. R. Chirieac, R. Kaur, A. Lightbown, J. Simendinger, T. Li, R. F. Padera, C. Garcia-Echeverria, R. Weissleder, U. Mahmood, L. C. Cantley, K. K. Wong, *Nat. Med.* **2008**, *14*, 1351 – 1356.
[26] A. D. Kohn, F. Takeuchi, R. A. Roth, *J. Biol. Chem.* **1996**, *271*, 21920 – 21926.

Received: March 25, 2015
Published online: May 7, 2015

